The University of Tehran Press

Pollution

Print ISSN: 2383-451X
Online ISSN: 2383-4501

https://jpoll.ut.ac.ir/

Lagrangian Model Analysis for Nuclear Materials Dispersion in Marine Environments (Persian Gulf)

Maryam Mohammadi[1] | Ahmad Pirouzmand[1,2] | Kamal Hadad[1,2]✉ | Abdorreza Alavi Gharahbagh[3]

1. Department of Nuclear Engineering, School of Mechanical Engineering, Shiraz University, P.O.Box 7193616548, Shiraz, Iran.
2. Safety Research Center, Shiraz University, P.O.Box 7193616548, Shiraz, Iran
3. Shahrood Branch, Islamic Azad University, P.O.Box 43189-36199, Shahrood, Iran

Article Info

Article type:
Research Article

Article history:
Received: 28 February 2025
Revised: 28 June 2025
Accepted: 6 September 2025

Keywords:
Radionuclide
Pollution
Nuclear accident
Transport model

ABSTRACT

This study analyzes the sensitivity of a Lagrangian model for the dispersion of nuclear materials in marine environments. The dispersion modeling of radionuclides in marine environments is a crucial step in an effective emergency preparedness and response (EPR) framework. The impact of number of particles, time step, and distance from the pollutant source on the output of the Lagrangian model was evaluated. According to the results, to keep the model's output unchanged when repeating the simulation, the initial number of particles must be at least 400,000. The minimum time step that maximizes accuracy is equal to the time step of the model's input data, but reducing the time step increases computational costs and execution time. Although distance from the pollution source did not significantly affect concentration levels, at grid points with high concentrations, the coefficient of variation was lower across different implementations, regardless of distance from the pollution source. To the best of the authors' knowledge, this study is the first sensitivity analysis of a Lagrangian model's parameters for radionuclide dispersion in the Persian Gulf.

Cite this article: Mohammadi, M., Pirouzmand, A., Hadad, K., & Alavi Gharahbagh, A. (2025). Lagrangian Model Analysis for Nuclear Materials Dispersion in Marine Environments (Persian Gulf). *Pollution*. 11(4), 1350-1362. https://doi.org/10.22059/poll.2025.391262.2821

 Publisher: The University of Tehran Press.
DOI: https://doi.org/10.22059/poll.2025.391262.2821

INTRODUCTION

Modeling is a useful tool for analyzing nuclear accidents and developing appropriate strategies for crisis management in the emergency, post-emergency, and long-term phases following a nuclear accident. With the expansion of nuclear power plants (NPPs) and nuclear facilities, assessing the risks associated with the contamination of radioactive substances has become a significant concern (Valizadeh et al., 2024). The assessments mainly depend on modeling and the quantity of radioactive material released during nuclear accidents. After the nuclear Fukushima and Chornobyl accidents, which released significant amounts of radioactive pollution into the soil, atmosphere, and water, several studies have been conducted to evaluate dispersion of the pollution in environments (Konoplev, 2022). The modeling approach depends on the source of pollution and the release environment. Marine environments are crucial in modeling the release of radioactive materials because nuclear power plants are typically situated nearby. Radioactive pollution in marine environments can occur indirectly through atmospheric deposition or directly into the water from discharges of nuclear waste and accidents near water environments and rivers (Livingston & Povinec, 2000; Rajkhowa et al., 2021).

*Corresponding Author Email: *hadadk@shirazu.ac.ir*

The study area is the Persian Gulf (PG), a warm sea in the Middle East. The depth of the PG increases from west to east, with an average depth ranging from 40 to 50 meters. The typical depth in the coastal area is between 18 and 20 meters (Vaughan et al., 2019). From a modeling perspective, the PG is classified as a shallow water environment, and this characteristic must be considered in modeling. The PG has unique characteristics that differentiate it from other global water and land areas, which gives it significant importance. It currently supplies 65% of the world's oil and contains nearly 30% of global natural gas reserves (Norouzi, 2020; Mohebbi-Nozar, 2022). The Bushehr and Barakah NPPs are located near the PG.

Given the importance of the PG, extensive research has been conducted on the radionuclide dispersion patterns after nuclear accidents. Most research has focused on the atmospheric distribution of pollutants (Feyzinejad et al., 2019; Alrammah et al., 2022; Alrammah, 2023; Lee et al., 2014; Pirouzmand et al., 2015 and 2018; Nabavi et al., 2023), while relatively few studies addressed the radionuclide dispersion in the PG. A CROM model was utilized to analyze long-term dispersion due to a direct release without accounting for tides and wind (Kamyab et al., 2018). Similarly, the CROM model was applied to investigate radionuclide release patterns in the PG (Hassanvand & Mirnejad, 2019). This study modeled wind under a hypothetical scenario; however, the effect of tides was not considered. A comprehensive 3D model for radionuclide dispersion in the PG was proposed incorporating the effects of wind and tides (Periáñez, 2021). This Lagrangian approach is designed to assess long-term dispersion patterns. A 2D Eulerian-Lagrangian SCHISM model was employed to simulate radioactive material transport in PG, considering tides and wind effects but excluding the impact of depth on wind-induced currents (Nesterov et al., 2023). The POSEIDON_R model was utilized to assess the long-term distribution of radionuclides, considering tides while disregarding wind-induced currents (Maderich et al., 2023).

Despite the development of various models for estimating the dispersion of nuclear pollutants in marine environments (Muhamad et al., 2024; Brovchenko et al., 2024), few studies have been conducted on the sensitivity analysis of radionuclide transport models (Kim et al., 2025; li et al., 2025). Some studies focused on the uncertainty of parameters related to nuclear accidents (Sadeghi et al., 2024; Hanfland et al., 2024; Nabavi et al., 2023), while a comprehensive analysis of the model's sensitivity has not been conducted.

Among the proposed methods for modeling the radionuclides dispersion in PG, the 3D model proposed in (Periáñez, 2021) demonstrates greater flexibility and efficiency than other models. The use of numerical solutions such as (Periáñez, 2021), rather than being restricted to general models such as CROM, SCHISM, and POSEIDON_R, allows users to independently analyze the impact of various parameters on pollution dispersion. Therefore, in this study, the Lagrangian model (Periáñez, 2021) was selected as the baseline model.

The aim of the current study is to analyze the effects of three key model parameters, including the number of particles (NPs), time step, and distance from the pollution source, on response accuracy and output stability. To the best of our knowledge, the current study is the first one that investigates the impact of the time step and NPs on execution time, memory usage, and final output of a Lagrangian transport model in PG. Moreover, the effect of distance from the pollution source on final output has been analyzed.

MATERIALS AND METHODS

In this section, the theory of Lagrangian transport model proposed by Periáñez explained, and implemented in the PG. Figure 1 illustrates the block diagram of the baseline. It involves several steps: First, input data, including source details and water current information are retrieved from relevant databases. Next, the initial positions, concentrations, and entry times of

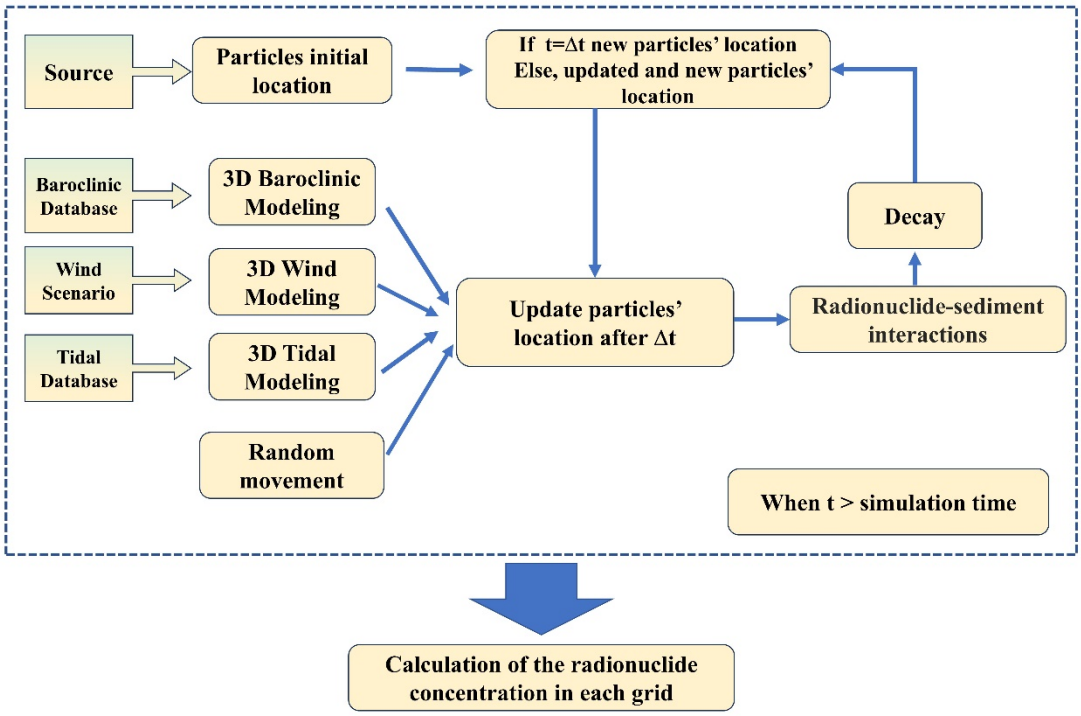

Fig. 1. The block diagram of the baseline for dispersion of radionuclides

the particles are calculated based on the source's parameters and location. At the start, the data for particles released at the initial time is integrated into the calculation cycle. The previous particles are updated with their new locations in subsequent time steps, and additional particles are introduced based on the release time pattern. Particle locations are updated using water current data, and a 3D random motion is applied to the particles. All particles also undergo decay and water-sediment interactions. This step calculates the 3D concentration of radionuclides and determines the concentration pattern in PG.

- *Water Currents Modeling (Baroclinic, Wind, and Tide)*

Periáñez utilized a database and hypothetical scenarios to model baroclinic and wind-induced currents, respectively (Periáñez, 2021). A model based on the harmonic analysis was employed to simulate tidal currents (Pous et. al., 2012). In the modifications made by Periáñez, the tidal model for the PG is considered as follows (Parker, 2007; Boon, 2013):

$$U(t) = H_0 + \sum_{i=1}^{5} G_i f_i \cos(\omega_i t - \varphi_i + V_i) \quad (1)$$

Where, H_0 is the residual current associated with the location, ω_i denotes the frequency of the corresponding component (given in (Periáñez, 2021)), G_i and φ_i are the adaptive amplitude and phase (in the local time meridian), respectively. These values are derived from analyzing tidal data in the PG. f_i is the nodal factor, and V_i is the equilibrium argument of the constituent at Greenwich. The $U(t)$ is the depth average of the tidal current at each point. f_i and V_i are measured from the beginning of the year, establishing the origin of time at the start of each year. In shallow waters, the profile of the tidal current components ($u_{tide}(z)$, $v_{tide}(z)$) near the bed is modeled using the power ($1/\alpha$) law (Soulsby, 1997):

$$u_t(z) = \left(\frac{z}{\beta h}\right)^{1/\alpha} U(t) \quad (2)$$

Where β is the bed roughness, z denotes height from sea bed, and h denotes the water depth.

- *Radionuclide Transport Modeling*

In the transport step of the baseline model, hypothetical radionuclide particles are released based on the temporal pattern of the pollution source. These particles then distribute based on water current and the other factors influencing their release in the marine environment. After a certain period, the activity per unit volume and distribution pattern can be calculated using these particles. Given that the pollution source is assumed to be known in the model, the primary particles have a specific and constant activity. In the baseline model, the calculation of horizontal and vertical movement caused by advection and diffusion, are considered as follows (Periáñez, 2005, 2021; Periáñez et al., 2019):

$$\begin{aligned} \Delta x &= u_{total}\Delta t + D_h Z_1 \cos(2\pi Z_2) \\ \Delta y &= v_{total}\Delta t + D_h Z_1 \sin(2\pi Z_2) \\ \Delta z &= \pm D_v \end{aligned} \tag{3}$$

Where Δx, Δy, and Δz represent the changes in particle location, u_{total} and v_{total} are the particle velocity components during a specific time step of Δt. Z_1 and Z_2 represent standard normal random variables with zero means and unit variances. D_h and D_v are respectively the maximum displacement of a particle in horizontal and vertical directions (Periáñez, 2005, 2021; Periáñez et al., 2019). After modeling the particle movements using the Lagrangian model, the processes of radioactive decay and water-sediment interactions are executed at each time step (Figure 1). During the decay process, the particle is entirely removed from the simulation. The probability of decay is (Periáñez, 2005, 2021; Periáñez et al., 2019):

$$p_d = 1 - e^{-\lambda\Delta t} \tag{4}$$

Where λ is the decay constant (10960 days for Cs-137). Periáñez has simulated water-sediment interactions with a one-step kinetic model (Periáñez, 2005, 2021; Periáñez et al., 2019). The modeling process is repeated with the time step Δt until the end of the simulation period.

- *Pollution Source*

In the Lagrangian model, pollution sources can be represented by direct point releases or distributed across various points on a grid. Periáñez modeled the source as a point source with a uniform release rate, which releases Cs-137 into the water over a short time relative to the simulation time (Periáñez, 2021). The release location of the particles is defined as a specific point, with a three-dimensional random displacement within a limited range from a central point (Bushehr NPP).

RESULTS AND DISCUSSIONS

In this section, we analyze the effects of the NPs, time step, and distance from the pollution source on the model's output, respectively. We considered the computational cost, memory consumption, and execution time as other important parameters. The implementations were

conducted using MATLAB 2024, adhering to the assumptions outlined in (Periáñez, 2021) (any modifications made to a parameter are explicitly noted). Given the presence of blocks representing random movement, water-sediment interactions, and decay (the stochastic processes) all implementations were executed ten times, and the results were averaged. The results are reported at 6 points with equal radial distances of 0.5˚ from each other, as illustrated in Figure 2.

Number of Particles

Figures 3-5 show the average concentration (AC) of radionuclides at the surface water, bottom water, and sediment, along with their standard deviations in terms of NPs. The time

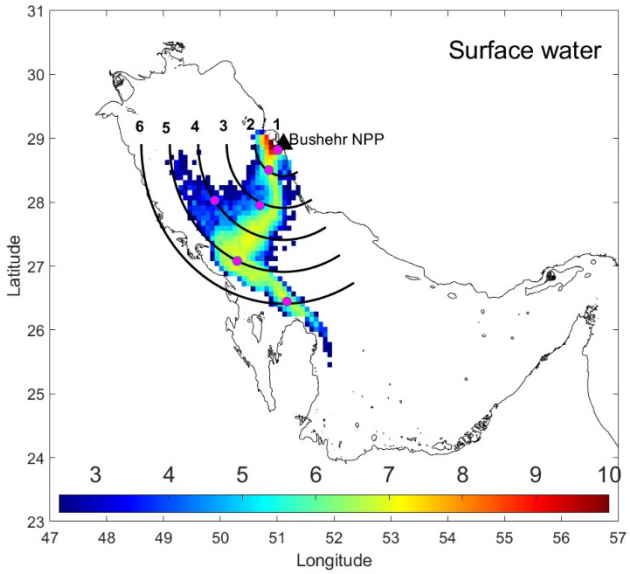

Fig. 2. The selected points for the analysis

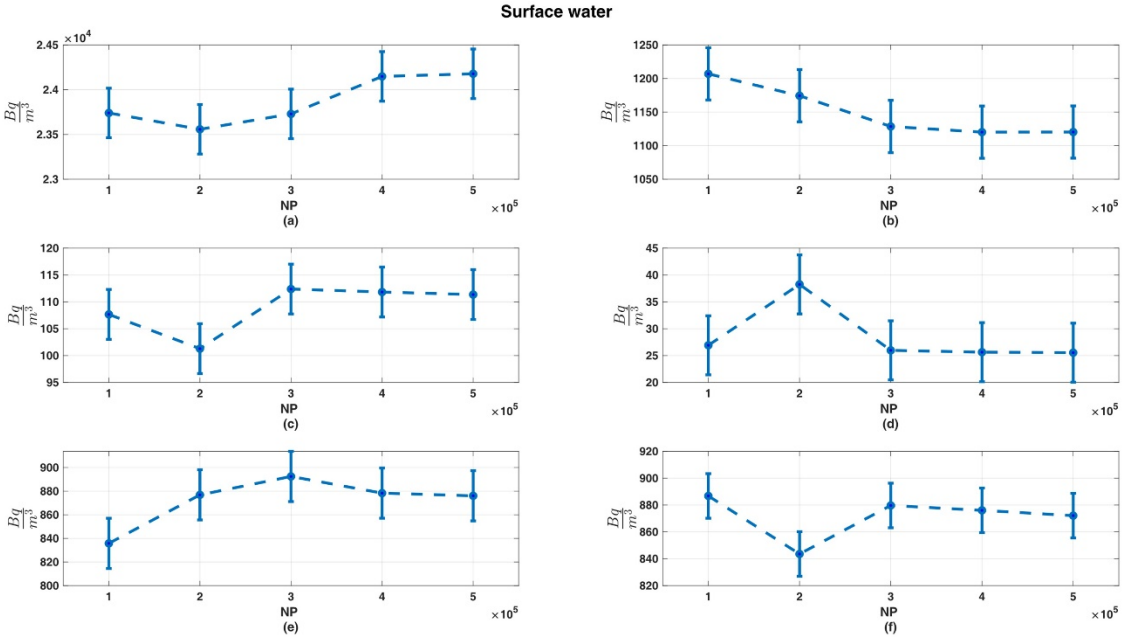

Fig. 3. The effect of NPs on ACs at surface water for: (a) point 1, (b) point 2, (c) point 3, (d) point 4, (e) point 5, and (f) point 6

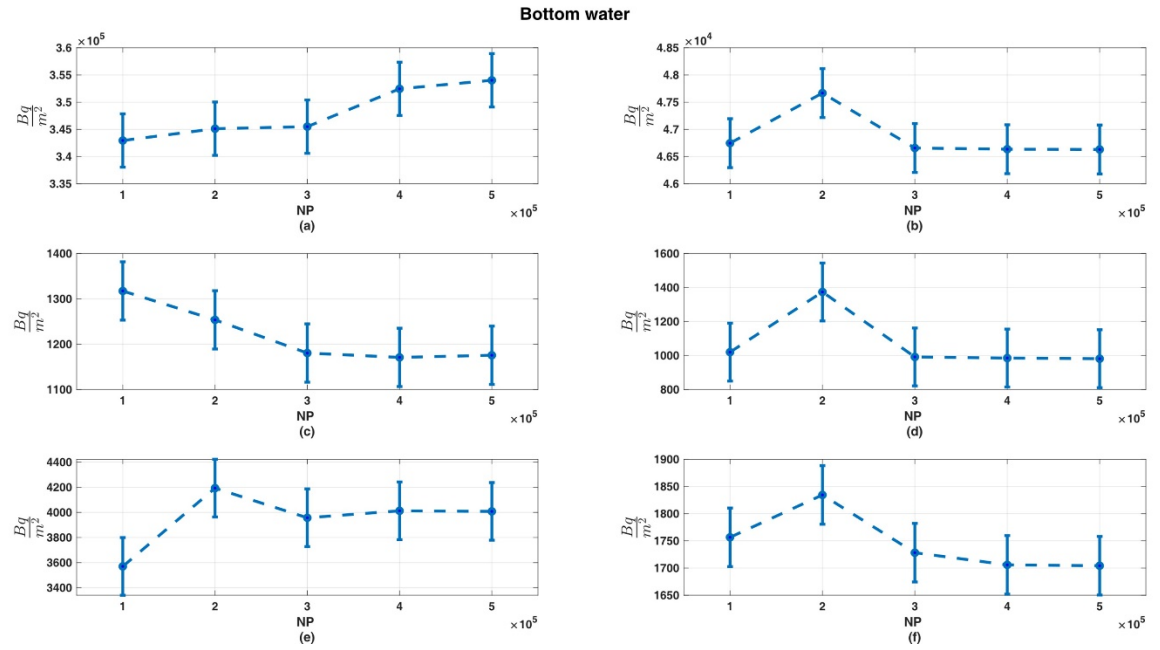

Fig. 4. The effect of NPs on ACs at bottom water for: (a) point 1, (b) point 2, (c) point 3, (d) point 4, (e) point 5, and (f) point 6

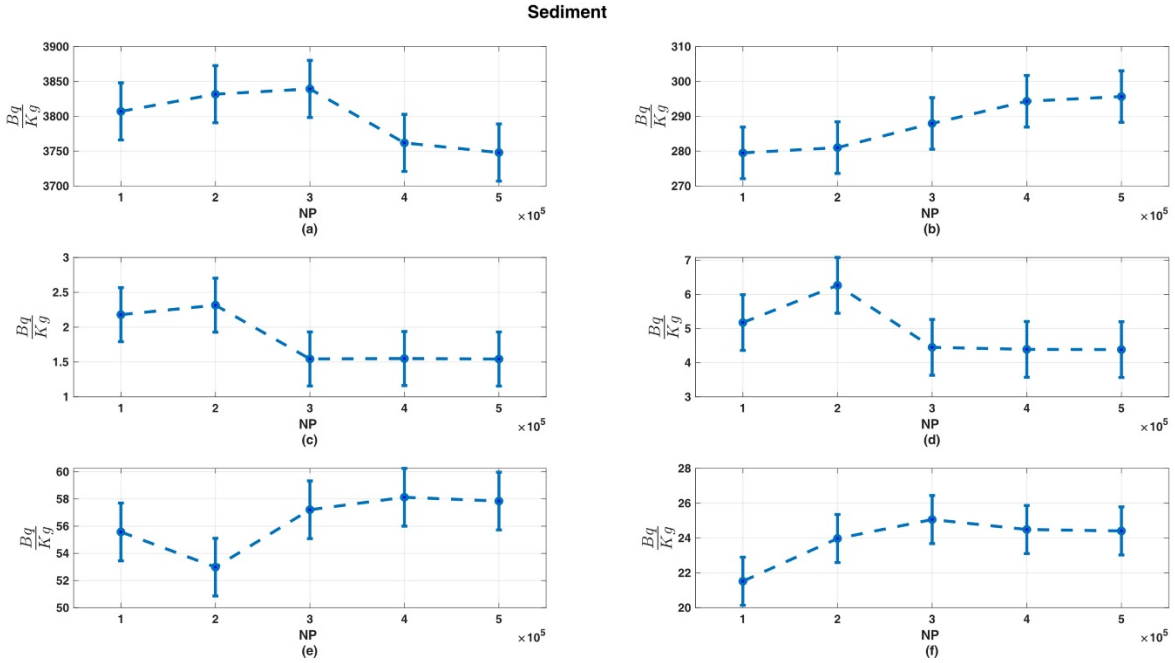

Fig. 5. The effect of NPs on ACs at sediment for: (a) point 1, (b) point 2, (c) point 3, (d) point 4, (e) point 5, and (f) point 6

step for all simulations was set at 600s. Average surface water, bottom water, and sediment concentrations are detailed in Table 1. As can be seen from Figures 3-5, the semi-constant standard deviation indicates that the effect of random parameters is independent of the NPs in each run, leading to the outcome fluctuations. However, results from 300,000 particles and above are more stable. Assuming a strict criterion includes points 1 and 2, both 400,000 and

Table 1. AC results for different NPs at the surface water (Bq/m^3), bottom water (Bq/m^2), and sediment (Bq/kg).

	NPs	Point 1	Point 2	Point 3	Point 4	Point 5	Point 6
Surface	100000	23740.29	1206.92	107.66	26.91	835.78	886.77
	200000	23557.55	1174.34	101.28	38.25	876.86	843.57
	300000	23729.43	1128.54	112.38	25.97	892.44	879.69
	400000	24222.84	1120.49	111.93	25.68	879.86	876.63
	500000	24212.65	1122.07	111.53	25.35	878.10	872.70
Bottom	100000	342951.49	46746.82	1317.41	1019.93	3569.77	1756.55
	200000	345125.92	47667.58	1253.67	1374.08	4193.06	1834.46
	300000	345501.31	46657.09	1180.48	991.60	3956.96	1728.22
	400000	352598.54	46647.19	1175.43	987.25	4010.23	1707.48
	500000	354247.74	46650.18	1178.53	985.48	4006.95	1704.55
Sediment	100000	3807.03	279.50	2.18	5.18	55.57	21.52
	200000	3831.68	281.00	2.32	6.27	52.99	23.97
	300000	3839.27	287.95	1.54	4.45	57.21	25.06
	400000	3763.44	294.35	1.55	4.45	58.24	24.56
	500000	3748.55	296.54	1.54	4.45	57.91	24.42

500,000 particles yield similar results. Thus, 400,000 was selected for the following simulations due to the lower computational cost.

Time Step

This section investigates the effect of Δt on the accuracy of the results. The value of Δt was constant in the baseline model, and in the current study, we analyzed the 300, 600, 1200, 1800, and 3600s. Figures 6-8 and Table 2 illustrate the AC obtained at the selected points. Based on the results shown in Figures 6-8, the AC remains constant with changes in Δt, while the standard deviation significantly increases as Δt increases. This shows that reducing computations by increasing the time step increases the effect of the model's random parameters on the output. Decreasing the time step does not enhance the accuracy of the input because monthly data was utilized in the baseline model, and linear regression was employed to generate data at smaller time steps. Since the random motion and the processes of water-sediment interactions and decay are repeated for each time step, reducing the time step increases the number of iterations of the random processes. Consequently, the average of these iterations is reflected in the final output, resulting in a reduced standard deviation of the final concentration across different runs. It is important to note that decreasing Δt directly leads to an increase in execution time, which is undesirable.

Distance from the Pollution Source

The AC is not an appropriate metric for evaluating the impact of distance from the pollutant source, since the final concentration of the radionuclide at a given location is directly affected by water currents during the simulation period. Additionally, the standard deviation between the results from different runs is not considered a reliable criterion, since it is directly related to the concentration at that location. Points with high concentrations, even with minor fluctuations, can result in a large standard deviation. For these reasons, the coefficient of variation (CV) has been employed to analyze the effect of distance from the pollution source. It is given by (Meeker et al, 2021):

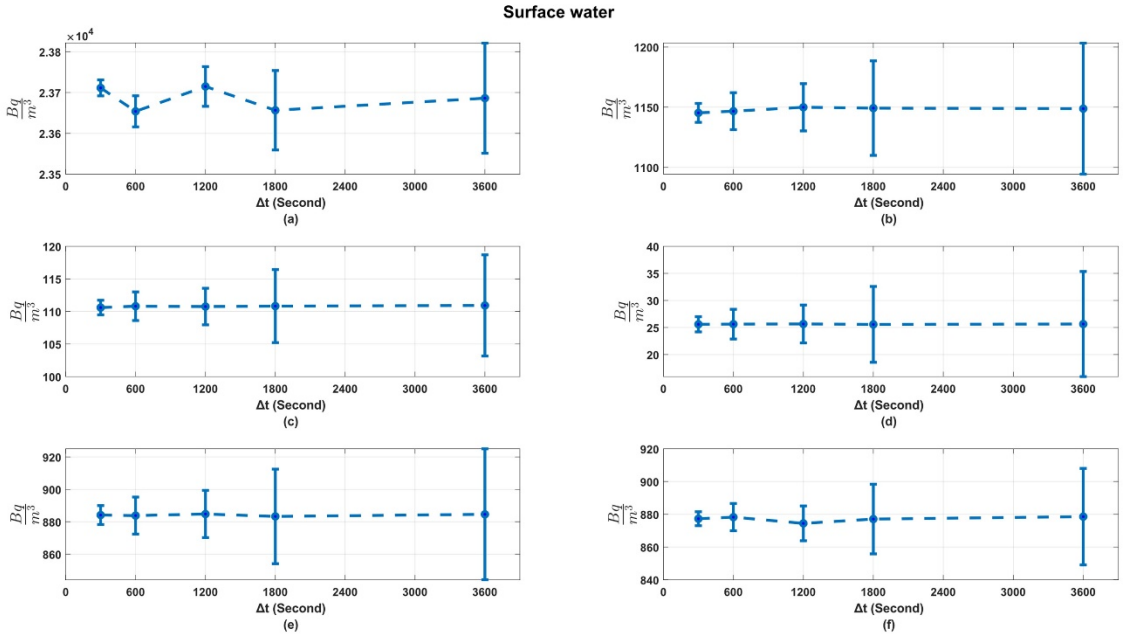

Fig. 6. The effect of time step on ACs at the surface water for: (a) point 1, (b) point 2, (c) point 3, (d) point 4 (e) point 5, and (f) point 6

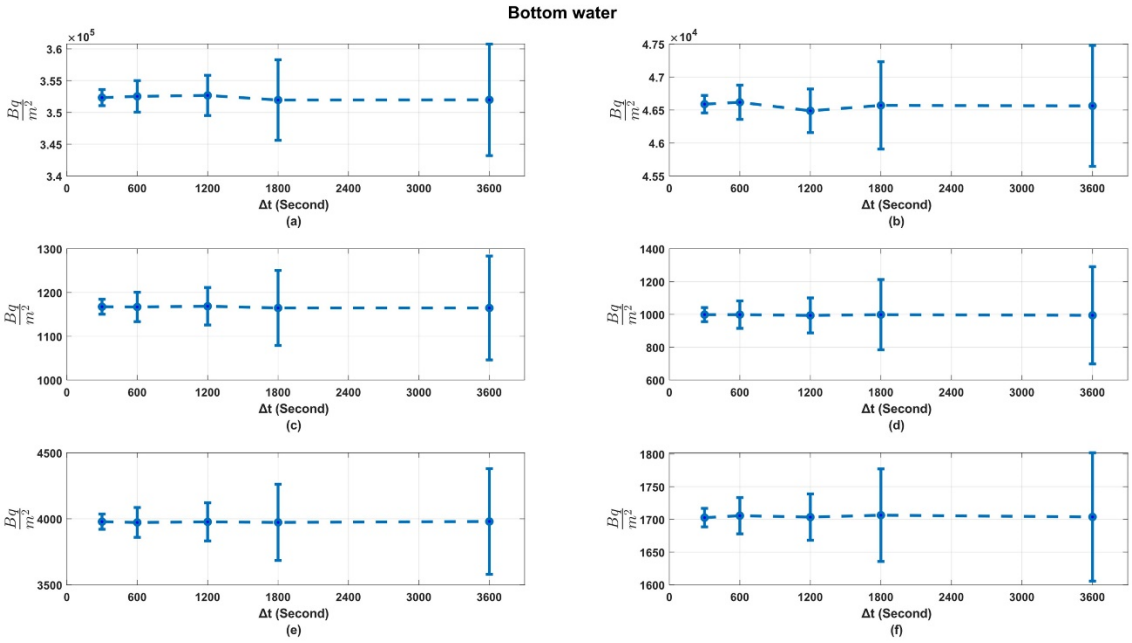

Fig. 7. The effect of time step on ACs at bottom water for: (a) point 1, (b) point 2, (c) point 3, (d) point 4, (e) point 5, and (f) point 6

$$CV=\sigma/\mu \quad (5)$$

Where σ and μ are the standard deviation and average of the results, respectively. This metric simultaneously considers the effects of standard deviation and average. Figure 9 illustrates the CVs for six points based on their distance from the source. As shown, no pattern can be observed. In Figure 10, instead of using distance from the source, the arrangement of points is based on

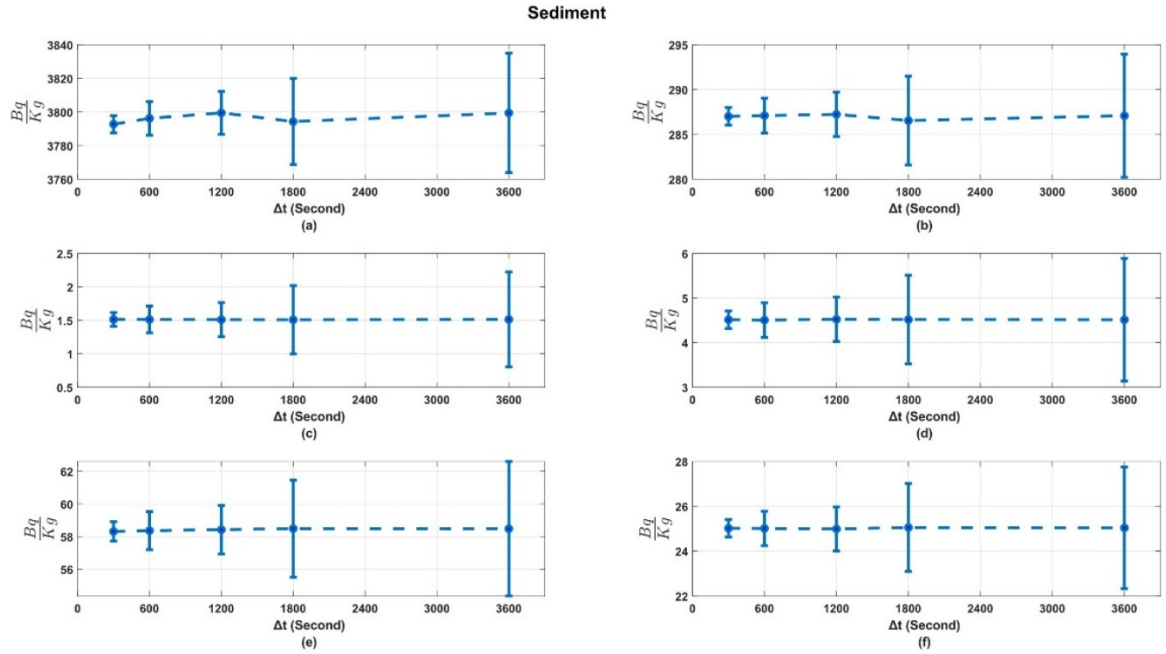

Fig. 8. The effect of time step on ACs at sediment for: (a) point 1, (b) point 2, (c) point 3, (d) point 4, (e) point 5, and (f) point 6

Table 2. AC results for different Δts at the surface water (Bq/m^3), bottom water (Bq/m^2), and sediment (Bq/kg).

	Δt (s)	Point 1	Point 2	Point 3	Point 4	Point 5	Point 6
Surface	300	23711.34	1145.29	110.60	25.59	884.15	877.30
	600	23653.90	1146.71	110.81	25.62	883.82	878.27
	1200	23714.81	1149.94	110.76	25.65	884.79	874.46
	1800	23656.53	1149.24	110.83	25.57	883.31	877.09
	3600	23686.13	1148.79	110.92	25.64	884.61	878.57
Bottom	300	352332.83	46588.90	1167.47	998.64	3977.93	1702.68
	600	352527.47	46617.66	1167.00	998.59	3972.16	1705.68
	1200	352675.72	46488.15	1168.62	993.82	3976.56	1703.53
	1800	351952.36	46569.93	1164.70	998.39	3972.72	1706.44
	3600	351982.66	46563.15	1164.66	994.41	3979.45	1703.75
Sediment	300	3792.74	287.01	1.51	4.51	58.31	25.02
	600	3796.23	287.10	1.51	4.51	58.36	25.01
	1200	3799.49	287.24	1.51	4.52	58.43	24.99
	1800	3794.32	286.55	1.51	4.52	58.49	25.05
	3600	3799.45	287.09	1.51	4.51	58.48	25.04

the average final concentration in descending order. The ACs and CVs for the selected points are detailed in Table 3. The results of Figure 10 and Table 3, clearly indicate that in cases where seawater currents move particles to specific locations, resulting in a high concentration at these points, the random parameters of the model exert less effect on the outcome. Consequently, the standard deviation of the average will be smaller.

Figure 11 shows the logarithm of the concentration after 90 days with the NP of 400,000. Other parameters were consistent with those in the baseline model (Periáñez, 2021). As shown, while the concentration is higher near the pollution source, a direct relationship between

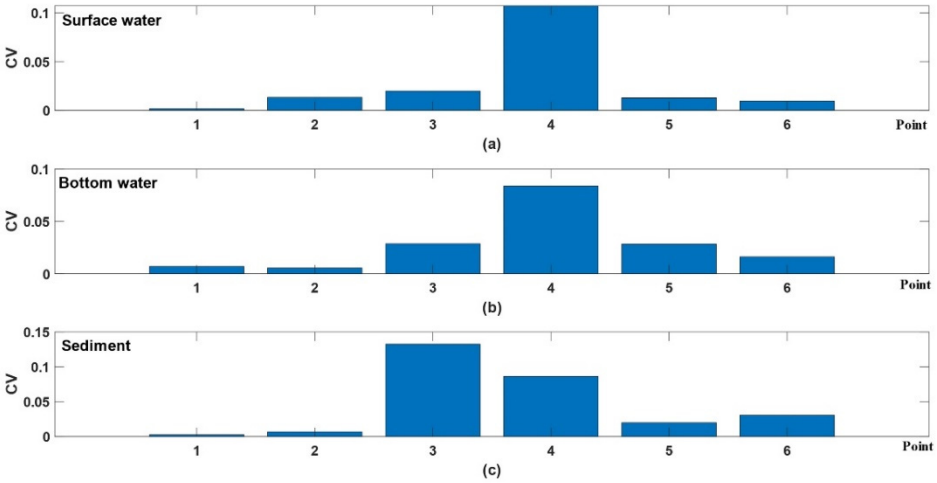

Fig. 9. Variation of CVs in terms of distance from the pollution source in: (a) surface water, (b) bottom water, and (c) sediment

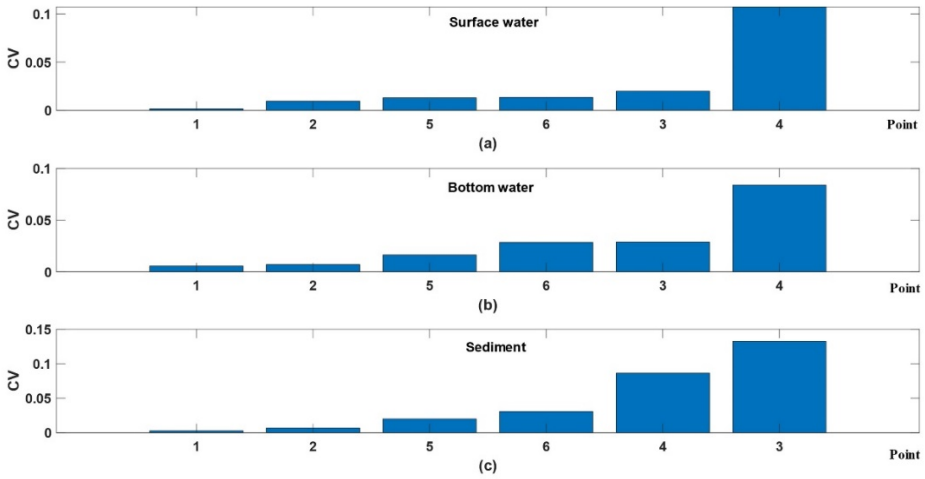

Fig. 10. Variation of CVs in terms of point concentration (descending) in: (a) surface water, (b) bottom water, and (c) sediment

Table 3. Results of CV and ACs at the surface water, bottom water, and sediment.

		point 1	**point 2**	**point 3**	**point 4**	**point 5**	**point 6**
Surface	AC (Bq/m3)	23653.90	1146.71	110.81	25.62	883.82	878.27
	CV	0.0016	0.0134	0.0198	0.1072	0.0129	0.0095
Bottom	AC (Bq/m2)	352527.47	46617.66	1167.00	998.59	3972.16	1705.68
	CV	0.0070	0.0056	0.0288	0.0839	0.0285	0.0163
Sediment	AC (Bq/kg)	3796.23	287.10	1.51	4.51	58.36	25.01
	CV	0.0026	0.0068	0.1325	0.0863	0.0200	0.0307

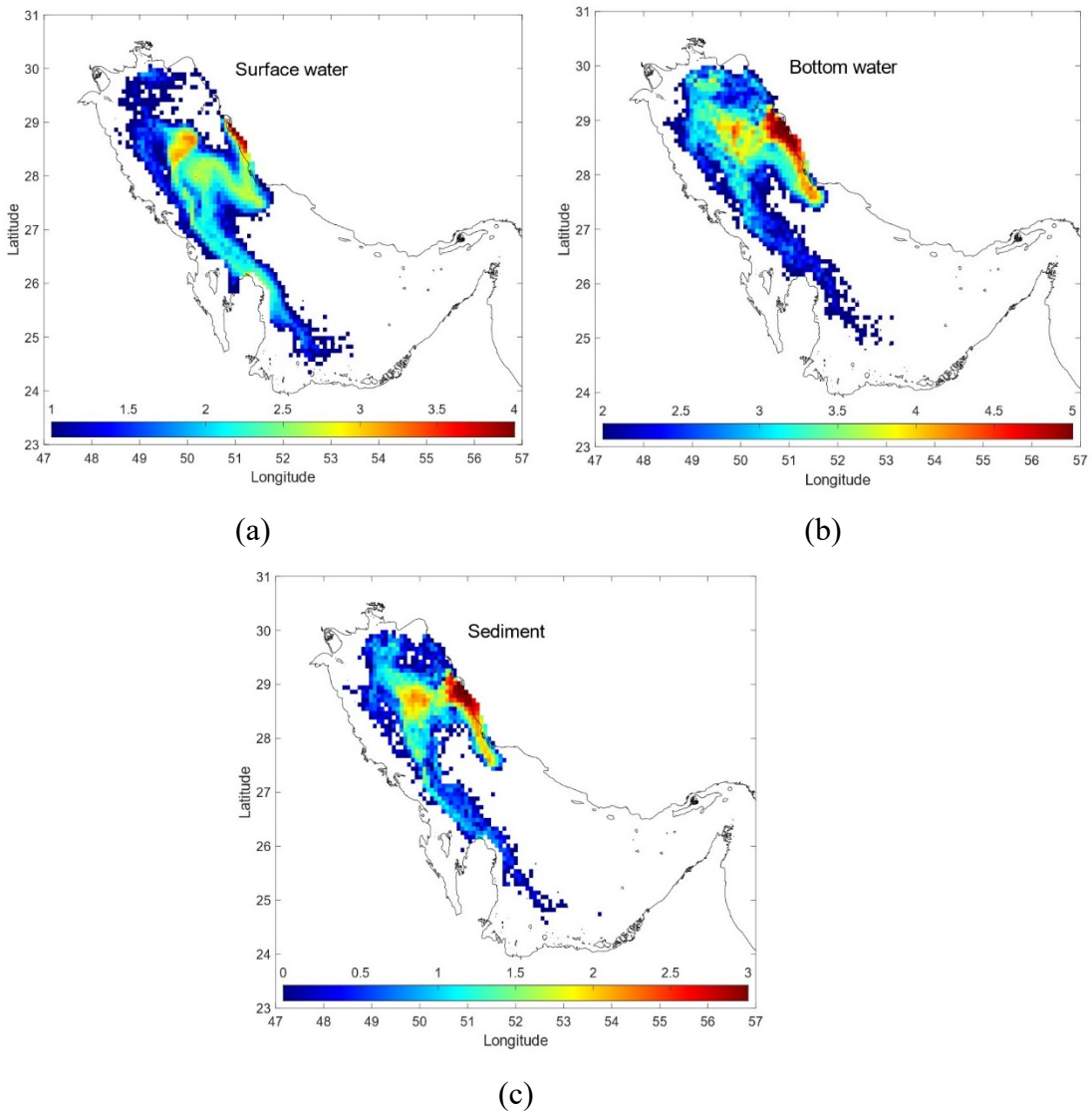

Table 3. Results of CV and ACs at the surface water, bottom water, and sediment.

concentration and distance from the pollution source cannot be established. This observation supports the assessment made in Figures 9 and 10.

CONCLUSIONS

This study analyzed the sensitivity of a Lagrangian transport model. The baseline model was Periáñez's framework which incorporates 3D baroclinic, tidal, and wind-induced currents and probabilistic mechanisms such as random movements, water-sediment interactions, and radioactive decay. Three unknown parameters that may affect the model's output have been assessed. These parameters were the NPs, time step, and distance from the pollution source. The results showed that the minimum NPs, needed to keep the model's output relatively unchanged, was 400,000. Increasing the NPs beyond this threshold increases computational cost, execution time, and memory requirements without improving the accuracy of the results. The minimum time step that maximized the response accuracy was equal to the time step of the input data. In fact, the time step is constrained by the temporal accuracy of the model input data. However, decreasing the time step (increasing time accuracy) mitigates the impact of random processes

on the output. A significant drawback of reducing the time step is the increase in computational costs and execution time. For the distance from the pollution source, the results did not show any relationship between distance and the output. Instead, it was demonstrated that in points with high concentrations, the CV was lower. In a real application, a trade-off between the required hardware and runtime constraints with the desired accuracy will determine the optimal values of NP and time step.

ACKNOWLEDGMENTS

The authors are thankful to Prof. Raúl Periáñez for sharing his transport model (APERTRACK).

GRANT SUPPORT DETAILS

The present research did not receive any financial support.

CONFLICT OF INTEREST

The authors declare that there is not any conflict of interests regarding the publication of this manuscript. In addition, the ethical issues, including plagiarism, informed consent, misconduct, data fabrication and/ or falsification, double publication and/or submission, and redundancy have been completely observed by the authors.

LIFE SCIENCE REPORTING

No life science threat was practiced in this research.

REFERENCES

Alrammah, I., Saeed, I. M. M., Mhareb, M. H. A., & Alotiby, M. (2022). Atmospheric dispersion modeling and radiological environmental impact assessment for normal operation of a proposed pressurized water reactor in the eastern coast of Saudi Arabia. Progress in Nuclear Energy, 145, 104121.

Alrammah, I. A. (2023). Analysis of nuclear accident scenarios and emergency planning zones for a proposed Advanced Power Reactor 1400 (APR1400). Nuclear Engineering and Design, 407, 112275.

Boon, J. D. (2013). Secrets of the tide: tide and tidal current analysis and predictions, storm surges and sea level trends. Elsevier.

Brovchenko, I., Kim, K. O., Maderich, V., Jung, K. T., & Kovalets, K. (2024). Lagrangian modelling of reactive contaminant transport in the multi-component marine medium. Computers & Geosciences, 187, 105579.

Feyzinejad, M., Malakooti, H., Sadrinasab, M., & Ghader, S. (2019). Radiological dose assessment by means of a coupled WRF-HYSPLIT model under normal operation of Bushehr nuclear power plant. *Pollution*, *5*(2), 429-448.

Hanfland, R., Pattantyús-Ábrahám, M., Richter, C., Brunner, D., & Voigt, C. (2024). The Lagrangian Atmospheric Radionuclide Transport Model (ARTM)—development, description and sensitivity analysis. *Air Quality, Atmosphere & Health*, *17*(6), 1235-1252.

Hassanvand, M., & Mirnejad, Z. (2019). Hydrodynamic model of radionuclide dispersion during normal operation and accident of Bushehr nuclear power plant. *Progress in Nuclear energy*, *116*, 115-123.

Kamyab, A., Torabi Azad, M., Sadeghi, M., & Akhound, A. (2018). Dispersion Simulation of Cesium 137 Released from a Hypothetical Accident at the Bushehr Nuclear Power Plant in Persian Gulf. *International Journal Of Coastal, Offshore And Environmental Engineering (ijcoe)*, *3*(3), 13-17.

Kim, H., Kim, K. O., Kim, S. Y., Suh, K. S., & Kwon, K. (2025). Dispersion behavior of Fukushima-derived 137Cs over the North Pacific with emphasis on its sensitivity to vertical velocity and

diffusion. *Marine Pollution Bulletin*, *212*, 117562.
Konoplev, A. (2022). Fukushima and Chernobyl: similarities and differences of radiocesium behavior in the soil–water environment. *Toxics*, *10*(10), 578.
Lee, J. K., Kim, J. C., Lee, K. J., Belorid, M., Beeley, P. A., & Yun, J. I. (2014). Assessment of wind characteristics and atmospheric dispersion modeling of 137Cs on the Barakah NPP area in the UAE. *Nuclear Engineering and Technology*, *46*(4), 557-568.
Li, H., Chen, D., Nie, B., & Wang, D. (2025). Numerical modeling and parameters analysis of marine radionuclide dispersion under the Fukushima Daiichi nuclear accident. *Progress in Nuclear Energy*, *184*, 105716.
Livingston, H. D., & Povinec, P. P. (2000). Anthropogenic marine radioactivity. *Ocean & Coastal Management*, *43*(8-9), 689-712.
Maderich, V., Bezhenar, R., Kovalets, I., Khalchenkov, O., & Brovchenko, I. (2023). Long-Term Contamination of the Arabian Gulf as a Result of Hypothetical Nuclear Power Plant Accidents. *Journal of Marine Science and Engineering*, *11*(2), 331.
Meeker, W. Q., Escobar, L. A., & Pascual, F. G. (2021). *Statistical methods for reliability data*. John Wiley & Sons.
Mohebbi-Nozar, S. L., Mortazavi, M. S., Seraji, F., & Bahreini, P. (2022). Health Risk Assessment of Okadaic Acid and Domoic Acid in some Edible Bivalves from Hormozgan Province in the North of Persian Gulf. *Pollution (2383451X)*, *8*(3).
Muhamad, L. H., Karim, M. K. A., Yusof, K. A., & Basri, N. A. (2024, May). Lagrangian and Eulerian approach to predict the movement of radionuclides in selected potential sites in Malaysia during the monsoon period. In *IOP Conference Series: Materials Science and Engineering* (Vol. 1308, No. 1, p. 012006). IOP Publishing.
Nabavi, S. O., Christoudias, T., Proestos, Y., Fountoukis, C., Al-Sulaiti, H., & Lelieveld, J. (2023). Spatiotemporal variation of radionuclide dispersion from nuclear power plant accidents using FLEXPART mini-ensemble modeling. *Atmospheric Chemistry and Physics*, *23*(13), 7719-7739.
Nesterov, O., Addad, Y., Bilal, S., Bosc, E., Abida, R., Al Shehhi, M. R., & Temimi, M. (2023). A numerical assessment of the dispersion of dissolved pollutants in the Arabian Gulf associated with the Barakah nuclear power plant. *Ocean Modelling*, *186*, 102274.
Norouzi, M. (2020). Evaluating the accumulation and consumption hazard risk of heavy metals in the fish muscles of species living in the waters of the Persian Gulf, Iran. *Pollution*, (4).
Parker, B. B. (2007). Tidal analysis and prediction.
Periáñez, R., Bezhenar, R., Brovchenko, I., Jung, K. T., Kamidara, Y., Kim, K. O., ... & Suh, K. S. (2019). Fukushima 137Cs releases dispersion modelling over the Pacific Ocean. Comparisons of models with water, sediment and biota data. *Journal of environmental radioactivity*, *198*, 50-63.
Periáñez, R. (2021). APERTRACK: A particle-tracking model to simulate radionuclide transport in the Arabian/Persian Gulf. *Progress in Nuclear Energy*, *142*, 103998.
Periáñez, R. (2005). *Modelling the dispersion of radionuclides in the marine environment*. Springer-Verlag Berlin Heidelberg.
Pirouzmand, A., Dehghani, P., Hadad, K., & Nematollahi, M. (2015). Dose assessment of radionuclides dispersion from Bushehr nuclear power plant stack under normal operation and accident conditions. International Journal of Hydrogen Energy, 40(44), 15198-15205.
Pirouzmand, A., Kowsar, Z., & Dehghani, P. (2018). Atmospheric dispersion assessment of radioactive materials during severe accident conditions for Bushehr nuclear power plant using HYSPLIT code. *Progress in Nuclear Energy*, *108*, 169-178.
Pous, S., Carton, X., & Lazure, P. (2012). A process study of the tidal circulation in the Persian Gulf. *Open Journal of Marine Science*, *2*(4), 131-140.
Rajkhowa, S., Sarma, J., & Das, A. R. (2021). Radiological contaminants in water: pollution, health risk, and treatment. In *Contamination of water* (pp. 217-236). Academic Press.
Sadeghi, K., Ghazaie, S. H., Stepanova, A., Sokolova, E., Modestov, V., Shirani, A., & Khoshmaram, M. (2024). Application of uncertainty and sensitivity analysis in dose assessment during a postulated LBLOCA for VVER-1000 nuclear reactor. *Nuclear Engineering and Design*, *421*, 113099.
Soulsby, R. (1997). Dynamics of marine sands. (London: Thomas Telford)
Valizadeh, B., Heydarizade, Y., Tayebi, J., & Rezaie, M. R. (2024). A Simulation to Assess the Probability of the Spread of Radioactive Materials from the Zaporizhzhia Nuclear Power Plant using the HYSPLIT Model. *Pollution*, *10*(1), 595-605.
Vaughan, G. O., Al-Mansoori, N., & Burt, J. A. (2019). The Arabian Gulf. In World Seas: *an Environmental Evaluation* (pp. 1–23). Elsevier.